

Research



Cite this article: Saxena P, Hossain M, Steinmann P. 2014 Nonlinear magneto-viscoelasticity of transversally isotropic magneto-active polymers. *Proc. R. Soc. A* **470**: 20140082.
<http://dx.doi.org/10.1098/rspa.2014.0082>

Received: 6 February 2014

Accepted: 11 March 2014

Subject Areas:

mechanical engineering, mathematical modelling, mechanics

Keywords:

magneto-viscoelasticity, nonlinear elasticity, viscoelasticity, transverse isotropy, magnetoelasticity

Author for correspondence:

Paul Steinmann

e-mail: paul.steinmann@ltm.uni-erlangen.de

Nonlinear magneto-viscoelasticity of transversally isotropic magneto-active polymers

Prashant Saxena, Mokarram Hossain
and Paul Steinmann

Chair of Applied Mechanics, University of Erlangen–Nuremberg,
Paul-Gordan Strasse 3, Erlangen 91052, Germany

Iron-filled magnetorheological polymers, when cured in the presence of a magnetic field, result in having a transversely isotropic structure with iron particles forming chains along the direction of applied magnetic induction. In this work, we model the magneto-viscoelastic deformation (and magnetization) process of such polymers. Components of the deformation gradient and the applied magnetic induction in the direction of anisotropy are considered to be additional arguments of the energy density function. The existence of internal damping mechanisms is considered by performing a multiplicative decomposition of the deformation gradient and an additive decomposition of the magnetic induction into equilibrium and non-equilibrium parts. Energy density functions and evolution laws of the internal variables are proposed that agree with the laws of thermodynamics. In the end, we present solutions of some standard deformation cases to illustrate the theory. In particular, it is shown that the orientation of resultant magnetic field and principal stress directions change with time owing to viscoelastic evolution.

1. Introduction

Magnetorheological elastomers (MREs) are materials in which the mechanical and magnetic responses have a strong nonlinear coupling with each other [1]. Usually, these are polymer-like soft materials used for variable mechanical behaviour in response to an applied magnetic field. MREs can be used as variable stiffness actuators and dampers [2–4], which have several potential

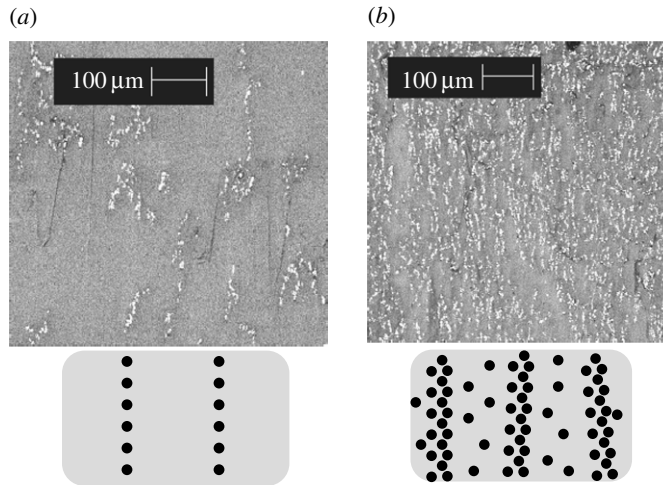


Figure 1. SEM images (Courtesy of Bastian Walter) and illustrative cartoon of MRE cured under a magnetic field in the vertical direction. Iron filler content: (a) 2% by volume and (b) 20% by volume.

engineering applications. Typically, these materials are made by curing a mixture of ferromagnetic particles (usually 1–5 μm in size) distributed in a polymeric matrix. Curing in the presence of a magnetic field causes the particles to form chain-like arrangements that imparts an effective directional anisotropy to the resulting polymer as can be seen from electron microscopy images in figure 1. Curing without a magnetic field results in an isotropic material [5,6]. When subjected to a magnetic field and mechanical loading, the magnetizable particles in the resulting polymer interact with each other and cause an increase in the overall stiffness of the material. This effect is more pronounced in the anisotropic materials when magnetization and mechanical loading are applied along the direction of particle chains [3].

Mathematical modelling of the coupling of mechanical and electromagnetic effects has been an interesting area of research in the past. Notable are the works of Landau & Lifshitz [7], Livens [8], Tiersten [9], Brown [10], Maugin & Eringen [11–13], Pao [14] and Eringen & Maugin [15]. Research in this field has accelerated in recent years mainly due to two reasons—firstly, the possibility of fabrication and testing of MREs in laboratories [2,3,5,6]; and secondly, further developments in the area of mathematical modelling and constitutive formulations, such as those by Brigadnov & Dorfmann [16], Dorfmann & Ogden [17] and Kankanala & Triantafyllidis [18]. In particular, the constitutive formulation of Dorfmann & Ogden [17,19] based on a ‘total’ energy density function has been helpful in the solution of several boundary value problems on nonlinear deformation and wave propagation [20–22]. It has been shown that any one of the magnetic induction, magnetic field or magnetization can be used as an independent input to the energy density function and the other two obtained through constitutive relations. We also mention the recent independent contributions of Steigmann [23] and Maugin [24] which discuss several issues concerning modelling the coupling of continuum magneto-electro-elasticity.

Based on Dorfmann and Ogden’s formulation, the authors of the present paper recently developed a mathematical model of large strain magneto-viscoelasticity [25]. In that work, we considered the possibilities of dissipation owing to mechanical viscoelasticity of the polymer matrix and to the resistance of the material to overall magnetization. We emphasize here that the overall magnetization of the material can occur not only due to the magnetization of individual (usually ferromagnetic) particles, but also due to the movement and realignment of these particles within the elastic matrix. This was affected in the model by a multiplicative decomposition of the deformation gradient into elastic and viscous parts ($\mathbf{F} = \mathbf{F}_e \mathbf{F}_v$) and an additive decomposition of the magnetic induction ($\mathbb{B} = \mathbb{B}_e + \mathbb{B}_v$)—the former based on the purely mechanical viscoelasticity theory [26,27]. A similar additive decomposition of the magnetization into a residual and a

reversible part has been considered by Maugin *et al.* [28] in order to model magnetomechanical hysteresis effects. Constitutive laws for material behaviour and evolution equations for \mathbf{F}_v and \mathbb{B}_v were proposed that are physically and thermodynamically consistent. In this paper, we extend this theory to model the rate-dependent properties of MREs with a directional anisotropy owing to particle chain alignment.

Modelling of soft elastomers with a directional anisotropy has been an active area of research in the recent times. One very common and useful method of doing so is to use the structural tensors, cf. Spencer [29] and Zheng [30]. By employing symmetry arguments, the energy function is considered to depend on scalar invariants of the right Cauchy–Green deformation tensor and the structure tensor defining anisotropy. This method has been employed by, among several other researchers, Shams *et al.* [31] for modelling pre-stressed elastic solids, Holzapfel & Gasser [32] for modelling fibre-reinforced composites, and Bustamante [33] and Danas *et al.* [34] for modelling transversally isotropic magneto-active elastomers. For the same class of methods, Shariff [35] presented a new set of invariants with immediate physical interpretation for fitting with experimental data; while Destrade *et al.* [36] discuss issues concerning the minimum number of invariants required in the energy density function for completeness, see also [37]. Recently, Srinivasa [38] has proposed a novel modelling method based on a decomposition of the deformation gradient into product of a rotation and an upper-triangular matrix.

Another approach for modelling anisotropic composite materials is to decouple the response of the matrix material and the anisotropy creating constituent (e.g. fibres for biological tissues, particle chains in our case). The two continua are nevertheless connected by the kinematic constraint of the same deformation gradient being applied to both. This procedure was used by Klinkel *et al.* [39] to model elasto-plasticity and was followed by Nedjar [40] in the modelling of viscoelastic deformation of anisotropic materials. We follow a similar approach with the additional constraint that along with the deformation gradient, the same magnetic induction applies to both the magnetoelastic matrix and the particle chains. The additive decomposition of energy leads to separated constitutive equations for the matrix and the chains which allows one to study the behaviour of each constituent separately. We take additional components of both the deformation gradient and the magnetic induction in the direction of particle chains and further decompose them into equilibrium and non-equilibrium parts to consider dissipation effects.

This paper is organized as follows. In §2, we present the basic kinematic relations required for the development of the theory. In this step, we define the components of the deformation gradient and the magnetic induction in the particle chain direction. Section 3 briefly presents the governing equations and the boundary conditions for a magnetoelastic problem. In §4, using a Clausius–Duhem form of the second law of thermodynamics, we derive the constitutive relations for stress and magnetic field as well as dissipation conditions that need to be satisfied by the time-evolution equations of the internal variables. As a simplification, the energy density is decomposed into equilibrium, non-equilibrium and anisotropic parts by taking motivation from experimental observations [6] and modelling considerations [40].

In §5, we specialize the material model to specific forms in order to obtain analytical and numerical solutions. Energy density functions for constitutive and evolution equations for internal variables are proposed, and stress and magnetic field are expressed in these specific forms. Some analytical solutions for the non-dissipative case under quasi-static loading conditions are presented in §6. In §7, we present numerical examples corresponding to three types of loading conditions—stationary pure shear, a time-dependent magnetic induction and a time-dependent strain. The obtained results for various material parameters and direction of applied loading with respect to the material anisotropy are presented graphically. Section 8 contains some brief concluding remarks.

2. Basic kinematics

Consider an incompressible magnetoelastic material which occupies the reference configuration \mathcal{B}_0 with a boundary $\partial\mathcal{B}_0$ in an unstressed state with no deformation. Upon a combined action

of mechanical boundary tractions and magnetic induction, the body is subjected to a static deformation and achieves a new spatial configuration. The spatial configuration and its boundary are denoted by \mathcal{B}_t and $\partial\mathcal{B}_t$, respectively, at time t . A deformation function χ can be defined such that it maps every point $\mathbf{X} \in \mathcal{B}_0$ to a point $\mathbf{x} = \chi(\mathbf{X}, t) \in \mathcal{B}_t$. The deformation gradient for the deformation process is defined as $\mathbf{F} = \text{Grad } \chi$, where Grad is the differential operator with respect to \mathbf{X} . Its determinant is given by $J = \det \mathbf{F}$ which is identically equal to unity in the case of incompressibility.

Let the direction of anisotropy given by a unit vector \mathbf{M} in \mathcal{B}_0 . After deformation, it is given by a vector $\mathbf{m} = \mathbf{F}\mathbf{M}$ in \mathcal{B}_t . Corresponding to the particle chain direction, it is now possible to define a chain deformation gradient $\mathbf{F}^c = \mathbf{m} \otimes \mathbf{M}$ capturing the one-dimensional deformation in the chain anisotropy direction. A definition of the structure tensor $\mathbf{G} = \mathbf{M} \otimes \mathbf{M}$ leads to the identity

$$\mathbf{F}^c = \mathbf{F}\mathbf{G}. \quad (2.1)$$

Thus, the tensor \mathbf{F}^c is simply a projection of \mathbf{F} in the direction of anisotropy. Henceforth, every quantity corresponding to the anisotropy in the chain direction is denoted with a superscript c . At this point, we also define the chain stretch in the particle chain direction to be given by $\lambda^c = |\mathbf{m}|$ such that the chain deformation gradient in (2.1) can be written as

$$\mathbf{F}^c = \lambda^c \hat{\mathbf{m}} \otimes \mathbf{M}, \quad (2.2)$$

where $\hat{\mathbf{m}}$ is the unit vector in the direction of \mathbf{m} . It is also noted that the tensor \mathbf{G} is idempotent, a property which will be useful later.

Let the magnetic induction be denoted by \mathbb{B} in \mathcal{B}_0 and \mathbb{b} in \mathcal{B}_t , related by the pullback operation $\mathbb{B} = J\mathbf{F}^{-1}\mathbb{b}$. We define a component of the magnetic induction in the chain direction to be given by a projection on the vector \mathbf{m} as $\mathbb{b}^c = [\mathbb{b} \cdot \hat{\mathbf{m}}]\hat{\mathbf{m}}$. Its Lagrangian form \mathbb{B}^c is given by the pullback operation $\mathbb{B}^c = J\mathbf{F}^{-1}\mathbb{b}^c$ as

$$\mathbb{B}^c = B^c \mathbf{M} \quad \text{and} \quad B^c = \frac{J[\mathbb{b} \cdot \hat{\mathbf{m}}]}{\lambda^c}. \quad (2.3)$$

In order to take into account mechanical viscous effects, we assume the existence of n imaginary intermediate configurations \mathcal{B}_i ($i = 1 \dots n$) that are related to \mathcal{B}_0 by a viscous motion and \mathcal{B}_t by a purely elastic deformation. The deformation routes through each of these \mathcal{B}_i are in parallel to the non-dissipative part of the magnetoelastic deformation from \mathcal{B}_0 to \mathcal{B}_t . This motivates the decomposition of the total deformation gradient into elastic and viscous parts (cf. [26,27]) as

$$\mathbf{F} = \mathbf{F}_e^i \mathbf{F}_v^i \quad \forall i = 1 \dots n. \quad (2.4)$$

In the interest of simplicity of analysis and notation, and without losing any mathematical rigour, we consider only one dissipative mechanism throughout this paper. However, we note that while proposing models to fit experimental data, one should work with the general case of multiple dissipative mechanisms. Thus, the above equation is simplified to

$$\mathbf{F} = \mathbf{F}_e \mathbf{F}_v. \quad (2.5)$$

As proposed by Nedjar [40] in the case of viscoelasticity, based on a similar treatment of elasto-plasticity by Klinkel *et al.* [39], we also perform a decomposition of the chain deformation gradient as

$$\mathbf{F}^c = \mathbf{F}_e^c \mathbf{F}_v^c, \quad (2.6)$$

$$= [\lambda_e^c \hat{\mathbf{m}} \otimes \mathbf{M}][\lambda_v^c \mathbf{M} \otimes \mathbf{M}], \quad (2.7)$$

where use has been made of equation (2.2) and we have performed a decomposition of the chain stretch as $\lambda^c = \lambda_e^c \lambda_v^c$.

An additive decomposition of the magnetic induction into equilibrium and non-equilibrium parts is done as shown in a previous paper [25]

$$\mathbb{B} = \mathbb{B}_e + \mathbb{B}_v. \quad (2.8)$$

Similar to the chain deformation gradient, we propose a decomposition of the chain magnetic induction \mathbb{B}^c into equilibrium and non-equilibrium parts as

$$\mathbb{B}^c = \mathbb{B}_e^c + \mathbb{B}_v^c, \quad (2.9)$$

and define the scalar equilibrium and non-equilibrium quantities B_e^c and B_v^c such that

$$B^c = B_e^c + B_v^c, \quad \mathbb{B}_e^c = B_e^c \mathbf{M} \quad \text{and} \quad \mathbb{B}_v^c = B_v^c \mathbf{M}. \quad (2.10)$$

For a later use, we define the right Cauchy–Green deformation tensors

$$\left. \begin{aligned} \mathbf{C} &= \mathbf{F}^t \mathbf{F}, & \mathbf{C}_e &= \mathbf{F}_e^t \mathbf{F}_e, & \mathbf{C}_v &= \mathbf{F}_v^t \mathbf{F}_v \\ \mathbf{C}^c &= (\mathbf{F}^c)^t \mathbf{F}^c, & \mathbf{C}_e^c &= (\mathbf{F}_e^c)^t \mathbf{F}_e^c & \text{and} & \mathbf{C}_v^c = (\mathbf{F}_v^c)^t \mathbf{F}_v^c. \end{aligned} \right\} \quad (2.11)$$

The left Cauchy–Green deformation tensor is given by $\mathbf{b} = \mathbf{F}\mathbf{F}^t$. As \mathbf{G} is idempotent, this gives

$$\mathbf{C}_v^c = (\lambda_v^c)^2 \mathbf{G}. \quad (2.12)$$

Furthermore, we present some identities for later use

$$\mathbf{C}^c = \mathbf{G}\mathbf{C}\mathbf{G}, \quad \frac{\partial \mathbf{C}^c}{\partial \mathbf{C}} = \mathbf{G} \otimes \mathbf{G} \quad \text{and} \quad \frac{\partial \mathbb{B}^c}{\partial \mathbb{B}} = \frac{1}{[\lambda^c]^2} \mathbf{G}\mathbf{C}. \quad (2.13)$$

3. Balance laws and boundary conditions for magnetoelasticity

It is assumed that the material is electrically non-conducting and that there are no electric fields. Let $\boldsymbol{\sigma}$ be the symmetric total Cauchy stress tensor that takes into account magnetic body forces (see, for example, [19] for its definition), ρ be the mass density, \mathbf{f}_m be the mechanical body force per unit volume, \mathbf{a} be the acceleration, \mathfrak{b} be the magnetic induction vector in \mathcal{B}_t and \mathfrak{h} be the magnetic field vector in \mathcal{B}_t . Then the following balance laws need to be satisfied in \mathcal{B}_t

$$\text{div } \boldsymbol{\sigma} + \mathbf{f}_m = \rho \mathbf{a}, \quad \boldsymbol{\sigma}^t = \boldsymbol{\sigma}, \quad \text{curl } \mathfrak{h} = \mathbf{0} \quad \text{and} \quad \text{div } \mathfrak{b} = 0. \quad (3.1)$$

Here, curl and div denote the corresponding operators with respect to \mathbf{x} in \mathcal{B}_t . Equation (3.1)₁ is the statement of balance of linear momentum, equation (3.1)₂ is the statement of balance of angular momentum, equation (3.1)₃ is a specialization of Ampère’s law and equation (3.1)₄ is the statement of impossibility of the existence of magnetic monopoles. It is important to note that in the case of problems studied here through magneto-mechanics, the speed of motions is much smaller than the speed of light c ; and the frequency of oscillations of all physical quantities is much smaller than the frequency of oscillation of electromagnetic fields involved in the propagation of a light wave. Thus, under these non-relativistic and ‘magnetostatic’ assumptions, the complete set of four Maxwell’s equations reduce to (3.1)_{3,4}. The magnetic vectors are connected through the standard constitutive relation

$$\mathfrak{b} = \mu_0 [\mathfrak{h} + \mathbf{m}], \quad (3.2)$$

where \mathbf{m} is the magnetization vector and μ_0 is the magnetic permeability of vacuum. If $\boldsymbol{\sigma}_{\text{mech}}$ is the purely mechanical stress tensor, then it is related to the total stress $\boldsymbol{\sigma}$ by the relation

$$\boldsymbol{\sigma} = \boldsymbol{\sigma}_{\text{mech}} + \frac{1}{\mu_0} \left[\mathfrak{b} \otimes \mathfrak{b} - \frac{1}{2} [\mathfrak{b} \cdot \mathfrak{b}] \mathbf{i} \right] + [\mathbf{m} \cdot \mathfrak{b}] \mathbf{i} - \mathfrak{b} \otimes \mathbf{m}. \quad (3.3)$$

Here \mathbf{i} is the second-order identity tensor in \mathcal{B}_t and use has been made of expression for the magnetic body force as $\mathbf{f} = [\text{grad } \mathfrak{b}]^t \mathbf{m}$; cf. [15] and the references therein.

The total Piola–Kirchhoff stress and the Lagrangian forms of \mathbb{h} , \mathbb{b} , \mathbb{b}^c and \mathbb{m} for an incompressible material are defined by using the pullback operations (cf. [19,41])

$$\mathbf{S} = J\mathbf{F}^{-1}\boldsymbol{\sigma}\mathbf{F}^{-t}, \quad \mathbb{H} = \mathbf{F}^t\mathbb{h}, \quad \mathbb{B} = J\mathbf{F}^{-1}\mathbb{b}, \quad \mathbb{B}^c = J\mathbf{F}^{-1}\mathbb{b}^c \quad \text{and} \quad \mathbb{M} = \mathbf{F}^t\mathbb{m}. \quad (3.4)$$

The above relations are used to rewrite the balance laws in \mathcal{B}_0 as

$$\text{Div}(\mathbf{S}\mathbf{F}^t) + \rho\mathbf{f}_m = \rho\mathbf{a}, \quad \mathbf{S}^t = \mathbf{S}, \quad \text{Curl } \mathbb{H} = \mathbf{0} \quad \text{and} \quad \text{Div } \mathbb{B} = 0, \quad (3.5)$$

along with the relation for magnetic quantities

$$J^{-1}\mathbf{C}\mathbb{B} = \mu_0[\mathbb{H} + \mathbb{M}]. \quad (3.6)$$

At a boundary $\partial\mathcal{B}_t$ which can be the bounding surface of the magnetoelastic body or a surface of discontinuity within the material, the following jump conditions need to be satisfied by the magnetic vectors

$$\mathbf{n} \times \llbracket \mathbb{h} \rrbracket = \mathbf{0} \quad \text{and} \quad \mathbf{n} \cdot \llbracket \mathbb{b} \rrbracket = 0. \quad (3.7)$$

Here, \mathbf{n} is the unit outward normal to $\partial\mathcal{B}_t$, and $\llbracket \bullet \rrbracket = \bullet^{\text{out}} - \bullet^{\text{in}}$ represents jump in a quantity across the boundary. The total Cauchy stress must satisfy

$$\boldsymbol{\sigma}\mathbf{n} = \mathbf{t}_a + \mathbf{t}_m, \quad (3.8)$$

where \mathbf{t}_a and \mathbf{t}_m are, respectively, the mechanical and magnetic contributions to the traction per unit area on $\partial\mathcal{B}_t$. In the reference configuration, the boundary conditions at the boundary $\partial\mathcal{B}_0$ are given by

$$\mathbf{N} \times \llbracket \mathbb{H} \rrbracket = \mathbf{0}, \quad \mathbf{N} \cdot \llbracket \mathbb{B} \rrbracket = 0 \quad \text{and} \quad \mathbf{F}\mathbf{S}\mathbf{N} = \mathbf{t}_a + \mathbf{t}_m, \quad (3.9)$$

where \mathbf{N} is the unit outward normal to $\partial\mathcal{B}_0$ and connected to \mathbf{n} through the Nanson's formula $\mathbf{n} \, da = J\mathbf{F}^{-t}\mathbf{N} \, dA$; da and dA being the current and the reference area elements, respectively. The vectors \mathbf{t}_a and \mathbf{t}_m are, respectively, the mechanical and magnetic contributions to the traction per unit area on $\partial\mathcal{B}_0$.

4. Thermodynamics and constitutive relations

We introduce a total energy density function similar to the one used by Dorfmann & Ogden [19] but generalized to also depend on the chain deformation tensor \mathbf{C}^c , the chain magnetic induction \mathbb{B}^c and the viscous variables \mathbb{C}_v^c , \mathbb{B}_v and \mathbb{B}_v^c , i.e.

$$\Omega(\mathbf{C}, \mathbf{C}^c, \mathbf{C}_v, \mathbf{C}_v^c, \mathbb{B}, \mathbb{B}^c, \mathbb{B}_v, \mathbb{B}_v^c). \quad (4.1)$$

The Clausius–Duhem form of the second law of thermodynamics is given as

$$-\dot{\Omega} + \frac{1}{2}\mathbf{S} : \dot{\mathbf{C}} + \mathbb{H} \cdot \dot{\mathbb{B}} \geq 0, \quad (4.2)$$

while the same for the case of incompressibility is

$$-\dot{\Omega} + \frac{1}{2}[\mathbf{S} + p\mathbf{C}^{-1}] : \dot{\mathbf{C}} + \mathbb{H} \cdot \dot{\mathbb{B}} \geq 0. \quad (4.3)$$

The Lagrange multiplier associated with the incompressibility constraint is given by p and henceforth we use a superposed dot to represent the material time derivative. On defining the velocity gradient tensor $\mathbf{l} = \dot{\mathbf{F}}\mathbf{F}^{-1}$, the rate of deformation tensor as its symmetric part as $\mathbf{d} = 1/2[\mathbf{l} + \mathbf{l}^t]$, and substituting in the above inequality, we can rewrite the above inequalities as

$$-\dot{\Omega} + \boldsymbol{\sigma} : \mathbf{d} + \mathbb{H} \cdot \dot{\mathbb{B}} \geq 0, \quad (4.4)$$

for a compressible material while for an incompressible material, we obtain

$$-\dot{\Omega} + [\boldsymbol{\sigma} + p\mathbf{i}] : \mathbf{d} + \mathbb{H} \cdot \dot{\mathbb{B}} \geq 0. \quad (4.5)$$

Here, \mathbf{i} is the identity tensor in \mathcal{B}_t .

On substituting the form of Ω from (4.1) into the above dissipation inequalities and using the standard Coleman–Noll procedure along with the identities in equation (2.13), we arrive at the following constitutive equations:

$$\mathbf{S} = 2 \frac{\partial \Omega}{\partial \mathbf{C}} + 2\mathbf{G} \frac{\partial \Omega}{\partial \mathbf{C}^c} \mathbf{G} \quad \text{and} \quad \mathbb{H} = \frac{\partial \Omega}{\partial \mathbb{B}} + \frac{1}{[\lambda^c]^2} \mathbf{G} \mathbf{C} \frac{\partial \Omega}{\partial \mathbb{B}^c}, \quad (4.6)$$

and a reduced form of the dissipation inequality

$$\frac{\partial \Omega}{\partial \mathbf{C}_v} : \dot{\mathbf{C}}_v + \frac{\partial \Omega}{\partial \mathbf{C}_v^c} : \dot{\mathbf{C}}_v^c + \frac{\partial \Omega}{\partial \mathbb{B}_v} \cdot \dot{\mathbb{B}}_v + \frac{\partial \Omega}{\partial \mathbb{B}_v^c} \cdot \dot{\mathbb{B}}_v^c \leq 0. \quad (4.7)$$

In the case of incompressibility, the constitutive equation (4.6)₁ is given by

$$\mathbf{S} = 2 \frac{\partial \Omega}{\partial \mathbf{C}} + 2\mathbf{G} \frac{\partial \Omega}{\partial \mathbf{C}^c} \mathbf{G} - p \mathbf{C}^{-1}. \quad (4.8)$$

It is noted in the above constitutive equations for stress and magnetic field that we get two components—one corresponding to the contribution from the isotropic matrix while the other coming from the particle chains. As $\mathbf{G} = \mathbf{M} \otimes \mathbf{M}$, the anisotropic components of stress and magnetic field (second term in equations (4.6)₁ and (4.6)₂) can be rewritten as

$$\mathbf{S}_{\text{aniso}} = 2 \left[\frac{\partial \Omega}{\partial \mathbf{C}^c} : \mathbf{G} \right] \mathbf{G} \quad \text{and} \quad \mathbb{H}_{\text{aniso}} = \frac{1}{[\lambda^c]^2} \left[\frac{\partial \Omega}{\partial \mathbb{B}^c} \cdot \mathbf{M} \right] \mathbf{C} \mathbf{M}. \quad (4.9)$$

These can be pushed forward to current configuration using the transformations $\boldsymbol{\sigma} = J^{-1} \mathbf{F} \mathbf{S} \mathbf{F}^t$ and $\mathbf{h} = \mathbf{F}^{-t} \mathbb{H}$ to give

$$\boldsymbol{\sigma}_{\text{aniso}} = 2J^{-1} \left[\frac{\partial \Omega}{\partial \mathbf{C}^c} : \mathbf{G} \right] \mathbf{m} \otimes \mathbf{m} \quad \text{and} \quad \mathbf{h}_{\text{aniso}} = \frac{1}{[\lambda^c]^2} \left[\frac{\partial \Omega}{\partial \mathbb{B}^c} \cdot \mathbf{M} \right] \mathbf{m}. \quad (4.10)$$

Thus, by definition, the principal component of the anisotropic part of the total stress and of the magnetic field lie in the direction of the particle chains \mathbf{m} .

From equation (2.12), we get the relation

$$\dot{\mathbf{C}}_v^c = 2\lambda_v^c \dot{\lambda}_v^c \mathbf{G}, \quad (4.11)$$

while from (2.10)₃, we obtain

$$\dot{\mathbb{B}}_v^c = \dot{B}_v^c \mathbf{M}, \quad (4.12)$$

and thus the inequality (4.7) can be expressed as

$$\frac{\partial \Omega}{\partial \mathbf{C}_v} : \dot{\mathbf{C}}_v + \frac{\partial \Omega}{\partial \mathbb{B}_v} \cdot \dot{\mathbb{B}}_v + 2\lambda_v^c \left[\frac{\partial \Omega}{\partial \mathbf{C}_v^c} : \mathbf{G} \right] \dot{\lambda}_v^c + \left[\frac{\partial \Omega}{\partial \mathbb{B}_v^c} \cdot \mathbf{M} \right] \dot{B}_v^c \leq 0. \quad (4.13)$$

Each one of the above expressions in (4.13) are of the form $\mathcal{F} \cdot \dot{\mathcal{I}}$ with \mathcal{F} being the driving force for the evolution of the internal variable \mathcal{I} . It is interesting to note that the driving forces for the internal variables \mathbf{C}_v and λ_v^c are similar to the expressions for isotropic and anisotropic parts of the stress in equations (4.6)₁ and (4.9)₁, and the same for \mathbb{B}_v and B_v^c are similar to the expressions for isotropic and anisotropic parts of the magnetic field in equations (4.6)₂ and (4.9)₂.

Using the relations $\mathbf{C}_v^c = [\lambda_v^c]^2 \mathbf{G}$, $\mathbb{B}_v^c = B_v^c \mathbf{M}$ and $\mathbf{G} : \mathbf{G} = \mathbf{M} \cdot \mathbf{M} = 1$, the last two expressions can be further simplified so that the above inequality (4.13) becomes

$$\frac{\partial \Omega}{\partial \mathbf{C}_v} : \dot{\mathbf{C}}_v + \frac{\partial \Omega}{\partial \mathbb{B}_v} \cdot \dot{\mathbb{B}}_v + \frac{\partial \Omega}{\partial \lambda_v^c} \dot{\lambda}_v^c + \frac{\partial \Omega}{\partial B_v^c} \dot{B}_v^c \leq 0. \quad (4.14)$$

(a) Magnetorheological elastomer preparation and some observations

In order to be able to provide physically reasonable models for anisotropic MREs, we prepare and analyse the samples for varying particle volume fractions. Iron particles coated with silicon-dioxide are mixed with ELASTOSIL and allowed to cure in the presence of a magnetic field for 16 h. Two different concentrations of 2 and 20% by volume of iron particles are taken. The cured samples are then analysed using scanning electron microscopy (SEM) images shown in figure 1.

It is observed that for low concentrations of 2%, the iron particles are able to form chain-like structures which are quite distinct from the elastomeric matrix. For a higher concentration of 20%, the particles do not just form chain-like structures but also disperse isotropically inside the matrix as shown in the accompanying cartoons in figure 1. These images are quite consistent with those obtained by, for example, Boczkowska & Awietjan [6].

These observations motivate the decomposition of the total free energy that is presented in §4*b*.

(b) Decomposition of free energy

The energy contribution from the homogeneous matrix is considered to be different from the contribution by the particle chains. Moreover, each one of them is also individually decomposed into equilibrium and non-equilibrium parts. Thus, we propose

$$\Omega = \Omega_e(\mathbf{C}, \mathbb{B}) + \Omega_{ec}(\mathbf{C}^c, \mathbb{B}^c) + \Omega_v(\mathbf{C}, \mathbf{C}_v, \mathbb{B}, \mathbb{B}_v) + \Omega_{vc}(\mathbf{C}^c, \mathbf{C}_v^c, \mathbb{B}^c, \mathbb{B}_v^c). \quad (4.15)$$

Here, Ω_e is the equilibrium magnetoelastic energy density of the homogeneous matrix, Ω_{ec} is the equilibrium anisotropic contribution due to the particle chains, Ω_v and Ω_{vc} are non-equilibrium parts of the isotropic and anisotropic energies, respectively.

For this decomposition of energy in equation (4.15), the total Piola–Kirchhoff stress and the magnetic field are given from (4.6) as

$$\mathbf{S} = 2 \frac{\partial \Omega_e}{\partial \mathbf{C}} + 2 \frac{\partial \Omega_v}{\partial \mathbf{C}} + 2\mathbf{G} \frac{\partial \Omega_{ec}}{\partial \mathbf{C}^c} \mathbf{G} + 2\mathbf{G} \frac{\partial \Omega_{vc}}{\partial \mathbf{C}^c} \mathbf{G} \quad (4.16)$$

and

$$\mathbb{H} = \frac{\partial \Omega_e}{\partial \mathbb{B}} + \frac{\partial \Omega_v}{\partial \mathbb{B}} + \frac{1}{[\lambda^c]^2} \left[\frac{\partial \Omega_{ec}}{\partial \mathbb{B}^c} \cdot \mathbf{M} \right] \mathbf{C}\mathbf{M} + \frac{1}{[\lambda^c]^2} \left[\frac{\partial \Omega_{vc}}{\partial \mathbb{B}^c} \cdot \mathbf{M} \right] \mathbf{C}\mathbf{M}. \quad (4.17)$$

For the case of incompressibility, the stress is given from (4.8) as

$$\mathbf{S} = -p\mathbf{C}^{-1} + 2 \frac{\partial \Omega_e}{\partial \mathbf{C}} + 2 \frac{\partial \Omega_v}{\partial \mathbf{C}} + 2\mathbf{G} \frac{\partial \Omega_{ec}}{\partial \mathbf{C}^c} \mathbf{G} + 2\mathbf{G} \frac{\partial \Omega_{vc}}{\partial \mathbf{C}^c} \mathbf{G}. \quad (4.18)$$

We note that, in general, the functional forms for Ω_e , Ω_v , Ω_{ec} and Ω_{vc} used in equations (4.16) and (4.18) will be different because they correspond to compressible and incompressible materials, respectively.

Remark 4.1. Normally, the isotropic matrix of a magneto-sensitive solid is made of rubber-like polymer material which, on its own, has no magnetic properties. However, in an iron-filled rubber cured in the presence of a magnetic field, the proportion of particles aligning to form particle chains largely depend on the volume fraction of the particles and type of base matrix, cf. figure 1 and the results of Boczkowska & Awietjan [6], for instance. For high volume fractions (approx. 20%) of iron particles, some particles align in chain like formations while the remaining are isotropically distributed in the matrix as shown in figure 1*b*. Thus, for this case, the entire material can be considered as magnetoelastic chains embedded in a magnetoelastic isotropic matrix and the decomposition of energy in equation (4.15) is reasonable. For very low volume fractions (approx. 2%) of iron particles, the structure can be considered to be that of a purely rubber matrix embedded with iron particle chains as shown in figure 1*a*. In this case, the isotropic equilibrium and non-equilibrium energies should be given by even simpler forms $\Omega_e(\mathbf{C})$ and $\Omega_v(\mathbf{C}, \mathbf{C}_v)$, respectively.

Remark 4.2. An alternative and useful approach towards writing the equilibrium part of energy has been given by Bustamante [33]. Using the theory of invariants, cf. Zheng [30], who shows that for a transversely isotropic magnetoelastic material the total equilibrium energy ($\Omega_e + \Omega_{ec}$ according to our definition) can be taken to depend on 10 invariants of \mathbf{C} , $\mathbb{B} \otimes \mathbb{B}$ and

$\mathbf{G} = \mathbf{M} \otimes \mathbf{M}$ given as

$$\left. \begin{aligned} I_1 &= \mathbf{C} : \mathbf{I}, & I_2 &= \frac{1}{2}[I_1^2 - \mathbf{C}^2 : \mathbf{I}], & I_3 &= \det \mathbf{C}, & I_4 &= [\mathbb{B} \otimes \mathbb{B}] : \mathbf{I}, \\ I_5 &= [\mathbb{B} \otimes \mathbb{B}] : \mathbf{C}, & I_6 &= [\mathbb{B} \otimes \mathbb{B}] : \mathbf{C}^2, & I_7 &= \mathbf{G} : \mathbf{C}, & I_8 &= \mathbf{G} : \mathbf{C}^2, \\ I_9 &= [\mathbb{B} \otimes \mathbb{B}] : \mathbf{G} & \text{and} & & I_{10} &= \mathbf{C}\mathbf{G}\mathbf{C} : [\mathbb{B} \otimes \mathbb{B}], \end{aligned} \right\} \quad (4.19)$$

where \mathbf{I} being the identity tensor in \mathcal{B}_0 . In this paper, however, we follow a different approach and separate the contribution arising owing to anisotropy as done in equation (4.15). Hence, only I_1, \dots, I_6 are used to define the isotropic part of free energy and the anisotropic part is written such that I_7, \dots, I_{10} are taken into account implicitly. This leads to simpler forms of energy density function as can be seen later and one can easily identify the isotropic and anisotropic contributions of the stress and the magnetic field. We believe that the present approach will lead to an easier identification of material parameters by correlation with experiments.

5. Specialized constitutive laws

We now consider some specialized form of energy density functions and evolution equations with a motivation to analyse the problem with analytical and numerical solutions. The material is considered to be incompressible henceforth.

(a) Energy density functions

For the equilibrium energy density corresponding to the isotropic matrix, we consider a functional form that is a generalization of the Mooney–Rivlin elastic solid to magnetoelasticity similar to the one used by Otténio *et al.* [21]

$$\Omega_e = \frac{\mu_e}{4} [[1 + \nu][I_1 - 3] + [1 - \nu][I_2 - 3]] + qI_4 + rI_6. \quad (5.1)$$

Here, μ_e is the shear modulus of material in the absence of any magnetic induction. The parameters q and r are magnetoelastic coupling constants with $q\mu_0$, $r\mu_0$ and ν being dimensionless, ν being restricted to the range $-1 \leq \nu \leq 1$ as for the classical Mooney–Rivlin model. We consider a similar functional form as above for the non-equilibrium part, albeit with non-equilibrium variables \mathbf{C}_v and \mathbb{B}_v .

$$\begin{aligned} \Omega_v &= \frac{\mu_v}{2} [\mathbf{C}_v^{-1} : \mathbf{C} - 3] + q_v [[\mathbb{B} - \mathbb{B}_v] \otimes [\mathbb{B} - \mathbb{B}_v]] : \mathbf{I} \\ &+ r_v [[\mathbf{C}[\mathbb{B} - \mathbb{B}_v]] \otimes [\mathbf{C}[\mathbb{B} - \mathbb{B}_v]]] : \mathbf{I}. \end{aligned} \quad (5.2)$$

This form was used by the authors in a previous work while modelling isotropic materials [25]. The parameters μ_v , q_v and r_v are viscous equivalents of the corresponding parameters in (5.1).

For the equilibrium energy density corresponding to the anisotropic part, we propose a one-dimensional form of the neo-Hookean function with an additional term to account for magnetic energy

$$\Omega_{ec} = \mu_e^c \left[[\lambda^c]^2 + \frac{2}{\lambda^c} - 3 \right] + \beta [\lambda^c]^4 [B^c]^2. \quad (5.3)$$

Here, λ^c is the stretch in the direction of chains as defined earlier in §2. The first term corresponds to an increase in the purely elastic energy due to the stretch λ^c with the elastic modulus μ_e^c while the second term (similar to the I_6 term in (5.1)) couples the deformation and magnetic induction in the anisotropy direction, β being a coupling parameter with dimensions of μ_0^{-1} . We consider a similar form of energy for the anisotropic non-equilibrium part as

$$\Omega_{vc} = \mu_v^c \left[[\lambda_e^c]^2 + \frac{2}{\lambda_e^c} - 3 \right] + \beta_v [\lambda^c]^4 [B^c - B_v^c]^2, \quad (5.4)$$

where μ_v^c and β_v are the viscous counterparts of the parameters in (5.3).

(b) Evolution laws

In order to complete the mathematical model of the material, we need to provide evolution laws for the non-equilibrium variables \mathbf{C}_v , \mathbf{C}_v^c , \mathbb{B}_v and \mathbb{B}_v^c which satisfy the dissipation inequality (4.14) and stop evolving if an equilibrium state is reached. Equilibrium in this case is defined by

$$\mathbf{C}_v = \mathbf{C}, \quad \lambda_v^c = \lambda^c, \quad \mathbb{B}_v = \mathbb{B} \quad \text{and} \quad B_v^c = B^c. \quad (5.5)$$

For the two variables \mathbf{C}_v and \mathbb{B}_v , we use the same evolution laws as used in the earlier work [25] because they satisfy the condition of thermodynamical consistency (4.14) as well as they stop evolution when equilibrium is reached. They are given by

$$\dot{\mathbb{B}}_v = \frac{\mu_0}{T_m} [q_v \mathbf{I} + r_v \mathbf{C}^2] [\mathbb{B} - \mathbb{B}_v] \quad \text{and} \quad \dot{\mathbf{C}}_v = \frac{1}{T_v} \left[\mathbf{C} - \frac{1}{3} [\mathbf{C} : \mathbf{C}_v^{-1}] \mathbf{C}_v \right]. \quad (5.6)$$

The evolution equation for \mathbf{C}_v has been used by Koprowski-Theiss *et al.* [42] and is based on a simpler form of that given by Lion [43].

For the internal variables corresponding to anisotropy (B_v^c and λ_v^c), we propose the following evolution laws:

$$\dot{B}_v^c = \frac{-1}{\beta_v T_m^c} \frac{\partial \Omega_{vc}}{\partial B_v^c} = \frac{1}{T_m^c} [\lambda^c]^4 [B^c - B_v^c] \quad (5.7)$$

and

$$\dot{\lambda}_v^c = \frac{-\lambda_v^c}{2\mu_v^c T_v^c} \frac{\partial \Omega_{vc}}{\partial \lambda_v^c} = \frac{1}{T_v^c} \left[\frac{[\lambda^c]^2}{[\lambda_v^c]^2} - \frac{\lambda_v^c}{\lambda^c} \right]. \quad (5.8)$$

In these equations, the parameters T_m , T_v , T_m^c and T_v^c are the specific relaxation times corresponding to each dissipation mechanism. For a simple case of constant deformation and magnetic induction (λ^c and B^c being constants), the evolution equation (5.7) can be integrated analytically to give

$$B_v^c = B^c \left[1 - \exp \left(- \frac{[\lambda^c]^4}{T_m^c} t \right) \right], \quad (5.9)$$

assuming $B_v^c = 0$ initially.

It is evident from the above equations that the thermodynamical inequality (4.14) is satisfied; equality occurring only when the equilibrium (5.5) is reached. The evolution laws are also physically consistent because evolution stops at the equilibrium (5.5)_{2,4} and the differential equations otherwise tend to evolve B_v^c and λ_v^c to approach the equilibrium values B^c and λ^c , respectively.

(c) Stress and magnetic-field calculations

For the given forms of energy density functions, the total Cauchy stress $\boldsymbol{\sigma} = \mathbf{FSF}^t$ is given in the following form

$$\boldsymbol{\sigma} = \boldsymbol{\sigma}_e + \boldsymbol{\sigma}_v + \boldsymbol{\sigma}_e^c + \boldsymbol{\sigma}_v^c - p\mathbf{i}, \quad (5.10)$$

where each of the above individual components are given as

$$\boldsymbol{\sigma}_e = \frac{\mu_e}{2} [[1 + \nu]\mathbf{b} + [1 - \nu][I_1 \mathbf{b} - \mathbf{b}^2]] + 2r\mathbb{b} \otimes [\mathbf{b}\mathbb{b}] + 2r[\mathbf{b}\mathbb{b}] \otimes \mathbb{b}, \quad (5.11)$$

$$\boldsymbol{\sigma}_v = \mu_v \mathbf{FC}_v^{-1} \mathbf{F}^t + 2r_v \mathbb{b}_e \otimes [\mathbf{b}\mathbb{b}_e] + 2r_v [\mathbf{b}\mathbb{b}_e] \otimes \mathbb{b}_e, \quad (5.12)$$

$$\boldsymbol{\sigma}_e^c = \left[\mu_e^c \left[1 - \frac{1}{[\lambda^c]^3} \right] + 2\beta [\lambda^c]^2 [B^c]^2 \right] \mathbf{g} \quad (5.13)$$

and

$$\boldsymbol{\sigma}_v^c = \left[\mu_v^c \left[\frac{1}{[\lambda_v^c]^2} - \frac{\lambda_v^c}{[\lambda^c]^3} \right] + 2\beta_v [\lambda^c]^2 [B^c - B_v^c]^2 \right] \mathbf{g}. \quad (5.14)$$

Here, we have defined the structure tensor of anisotropy in \mathcal{B}_t as $\mathbf{g} = \mathbf{F}\mathbf{G}\mathbf{F}^t$ and used the formula for the derivative with respect to $\mathbf{C}^c = [\lambda^c]^2\mathbf{G}$ as

$$\frac{\partial\Omega}{\partial\mathbf{C}^c} = \frac{1}{2\lambda^c} \frac{\partial\Omega}{\partial\lambda^c} \mathbf{G}. \quad (5.15)$$

The magnetic field $\mathbf{h} = \mathbf{F}^{-t}\mathbb{H}$ is given as

$$\mathbf{h} = \mathbf{h}_e + \mathbf{h}_v + \mathbf{h}_e^c + \mathbf{h}_v^c, \quad (5.16)$$

where each of the individual components are given by the following expressions

$$\mathbf{h}_e = 2q\mathbf{b}^{-1}\mathbb{b} + 2r\mathbf{b}\mathbb{b}, \quad (5.17)$$

$$\mathbf{h}_v = 2q_v\mathbf{b}^{-1}\mathbb{b}_e + 2r_v\mathbf{b}\mathbb{b}_e, \quad (5.18)$$

$$\mathbf{h}_e^c = 2\beta[\lambda^c]^2 B^c \mathbf{m} \quad (5.19)$$

and

$$\mathbf{h}_v^c = 2\beta_v[\lambda^c]^2 B_e^c \mathbf{m}. \quad (5.20)$$

Here, we have used the relation $\mathbf{m} = \mathbf{F}\mathbf{M}$.

It is worth noting the additional components here that arise owing to the directional anisotropy of the material (in comparison to eqns (47)–(51) of [25]). Both the total stress and the magnetic field have equilibrium and non-equilibrium terms in the direction of anisotropy.

6. Quasi-static loading conditions

In this section, we consider quasi-static changes in the deformation \mathbf{F} and the magnetic induction \mathbb{B} such that the non-equilibrium energies Ω_v and Ω_v^c remain identically zero. Equilibrium stress and equilibrium magnetic field are calculated for this case to understand the effects of directional anisotropy. We discuss two examples corresponding to uniaxial tension and simple shear in cartesian coordinates.

(a) Uniaxial tension, equilibrium solution

For the first case, a uniaxial deformation and a magnetic induction is applied in the direction of particle chain alignment. Let, $\mathbf{M} = \{1, 0, 0\}^t$, $\mathbb{B} = \{B_1, 0, 0\}^t$ and $\mathbf{F} = \text{diag}(\lambda, \lambda^{-1/2}, \lambda^{-1/2})$. For this deformation and magnetic induction, the principal components are given by $B^c = B_1$ and $\lambda^c = \lambda$, and the principal stress in the chain direction is

$$\sigma_{11} = \frac{\mu_e}{2} \left[[1 + \nu] \left[\lambda^2 - \frac{1}{\lambda} \right] + [1 - \nu] \left[\lambda - \frac{1}{\lambda^2} \right] \right] + \mu_e^c \left[\lambda^2 - \frac{1}{\lambda} \right] + 4r\lambda^4 B_1^2 + 2\beta\lambda^4 B_1^2. \quad (6.1)$$

The magnetic field $\mathbf{h} = \{h_1, h_2, h_3\}^t$ in this principal direction is given as

$$h_1 = 2 \left[\frac{q}{\lambda} + [r + \beta]\lambda^3 \right] B_1. \quad (6.2)$$

For this simple case of deformation and magnetization, the anisotropic component of energy provides a simple increment in the values of stress and magnetic field. The presence of parameter μ_e^c increases the effective value of the ‘mechanical’ shear modulus by linearly combining with μ_e while the parameter β increases the effective value of magnetic stress and magnetic field by linearly combining with r .

We now consider a different case in which the magnetic induction and the applied uniaxial deformation are perpendicular to the particle chain direction. Thus, $\mathbf{M} = \{0, 1, 0\}^t$, $\mathbb{B} = \{B_1, 0, 0\}^t$ and $\mathbf{F} = \text{diag}(\lambda, \lambda^c, [\lambda\lambda^c]^{-1})$. In this case, $B^c = 0$ and one needs to compute λ^c along with the

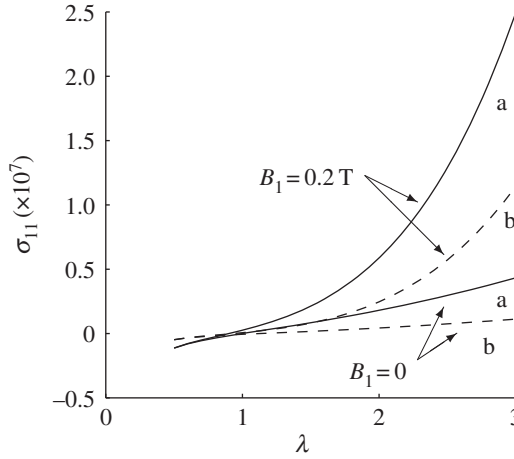


Figure 2. Stress σ_{11} (N m^{-2})—stretch λ plot for uniaxial deformation for two different values of magnetic induction. (a) $\mathbf{M} \parallel \mathbb{B}$ and (b) $\mathbf{M} \perp \mathbb{B}$.

Lagrange multiplier p . These are obtained by solving the set of simultaneous equations

$$\sigma_{22} = 0 = \frac{\mu_e}{2} \left[[1 + \nu][\lambda^c]^2 + [1 - \nu] \left[\lambda \lambda^c \right]^2 + \frac{1}{\lambda^2} \right] + \mu_e^c \left[[\lambda^c]^2 - \frac{1}{\lambda^c} \right] - p \quad (6.3)$$

and

$$\sigma_{33} = 0 = \frac{\mu_e}{2} \left[\frac{1 + \nu}{[\lambda \lambda^c]^2} + [1 - \nu] \left[\frac{1}{\lambda^2} + \frac{1}{[\lambda^c]^2} \right] \right] - p. \quad (6.4)$$

The expressions for λ^c and p can be computed from equations above and are too big to reproduce here. They can be substituted below to obtain the value of σ_{11} as

$$\sigma_{11} = \frac{\mu_e}{2} \left[[1 + \nu] \left[\lambda^2 - \frac{1}{[\lambda \lambda^c]^2} \right] + [1 - \nu] \left[[\lambda^c]^2 + \frac{1}{[\lambda \lambda^c]^2} - \frac{1}{\lambda^2} - \frac{1}{[\lambda^c]^2} \right] \right] + 4r\lambda^4 B_1^2. \quad (6.5)$$

The magnetic field is simply given by

$$h_1 = 2 \left[\frac{q}{\lambda} + r\lambda^3 \right] B_1. \quad (6.6)$$

In the absence of anisotropy, we have $\lambda^c = 1/\lambda^{1/2}$, $\beta = 0$ and the two expressions in (6.1) and (6.5) become the same. We also observe the mechanical and magnetic stress additions to σ_{11} and additional contribution to magnetic field owing to anisotropy by comparing the two expressions in (6.1), (6.5) and (6.2), (6.6).

Variation of stress σ_{11} with λ and B_1 for the two cases discussed above is shown in figure 2 for the following material constants:

$$\left. \begin{aligned} \mu_0 &= 4\pi \times 10^{-7} \text{ N A}^{-2}, & \mu_e &= 2.6 \times 10^5 \text{ N m}^{-2}, & \nu &= 0.3, \\ \mu_e^c &= 3 \times 10^5 \text{ N m}^{-2} & q &= r = \frac{1}{\mu_0} & \text{and} & \beta = \frac{2}{\mu_0}. \end{aligned} \right\} \quad (6.7)$$

The value of μ_e is taken to be the shear modulus at zero magnetic field for an elastomer filled with 10% by volume of iron particles, cf. Jolly *et al.* [5]. Values of ν, q, r are what have been used by Otténio *et al.* [21] and Saxena & Ogden [22]. The parameters μ_e^c and β are introduced in this paper and they being chain counterparts of μ_e and r , have been assigned values with the same order of magnitude.

In general, a larger magnetic field leads to an increase in the stress which is to be expected. For both extension and compression, a higher stress is achieved when magnetic induction is applied in the direction of chain anisotropy than when it is applied perpendicular to the chain direction.

(b) Simple shear, equilibrium solution

Let the particle chain be initially aligned along the x_2 direction such that $\mathbf{M} = \{0, 1, 0\}^t$. The material is sheared in the (1, 2) plane such that the deformation gradient and the various powers of the left Cauchy–Green deformation tensor are given by

$$[\mathbf{F}] = \begin{bmatrix} 1 & \gamma & 0 \\ 0 & 1 & 0 \\ 0 & 0 & 1 \end{bmatrix}, \quad [\mathbf{b}] = \begin{bmatrix} 1 + \gamma^2 & \gamma & 0 \\ \gamma & 1 & 0 \\ 0 & 0 & 1 \end{bmatrix} \quad (6.8)$$

and

$$[\mathbf{b}^2] = \begin{bmatrix} \gamma^2 + [1 + \gamma^2]^2 & 2\gamma + \gamma^3 & 0 \\ 2\gamma + \gamma^3 & 1 + \gamma^2 & 0 \\ 0 & 0 & 1 \end{bmatrix}, \quad [\mathbf{b}^{-1}] = \begin{bmatrix} 1 & -\gamma & 0 \\ -\gamma & 1 + \gamma^2 & 0 \\ 0 & 0 & 1 \end{bmatrix}. \quad (6.9)$$

In the first case, we consider a magnetic induction applied in x_2 direction given by $\mathbb{B} = \{0, B_2, 0\}^t$, which for the given deformation gives $\mathbb{b} = \{\gamma B_2, B_2, 0\}^t$. The components in the chain direction are given by $\lambda^c = \sqrt{1 + \gamma^2}$ and $B^c = B_2$. The structure tensor is given as

$$[\mathbf{g}] = \begin{bmatrix} \gamma^2 & \gamma & 0 \\ \gamma & 1 & 0 \\ 0 & 0 & 0 \end{bmatrix}. \quad (6.10)$$

For these loading conditions, the Lagrange multiplier is obtained by setting $\sigma_{33} = 0$ as

$$p = \frac{\mu_e}{2} [[1 + \nu] + [1 - \nu][2 + \gamma^2]]. \quad (6.11)$$

Thus, the various components of stress are obtained as

$$\sigma_{11} = \frac{\mu_e}{2} [1 + \nu] \gamma^2 + \mu_e^c \left[1 - \frac{1}{[1 + \gamma^2]^{3/2}} \right] \gamma^2 + 4r[2 + \gamma^2] \gamma^2 B_2^2 + 2\beta[1 + \gamma^2] \gamma^2 B_2^2, \quad (6.12)$$

$$\sigma_{22} = -\frac{\mu_e}{2} [1 - \nu] \gamma^2 + \mu_e^c \left[1 - \frac{1}{[1 + \gamma^2]^{3/2}} \right] + 4r[1 + \gamma^2] B_2^2 + 2\beta[1 + \gamma^2] B_2^2 \quad (6.13)$$

$$\text{and } \sigma_{12} = \mu_e \gamma + \mu_e^c \left[1 - \frac{1}{[1 + \gamma^2]^{3/2}} \right] \gamma + 2r[1 + 3\gamma^2 + \gamma^4] \gamma B_2^2 + 2\beta[1 + \gamma^2] \gamma B_2^2. \quad (6.14)$$

The expression for the components of magnetic field $\mathbb{h} = \{h_1, h_2, h_3\}^t$ in this case is given by

$$h_1 = 2r\gamma[2 + \gamma^2] B_2 + 2\beta\gamma[1 + \gamma^2] B_2 \quad (6.15)$$

and

$$h_2 = 2qB_2 + 2r[1 + \gamma^2] B_2 + 2\beta[1 + \gamma^2] B_2. \quad (6.16)$$

Now consider a case where the magnetic induction is applied in x_1 direction given by $\mathbb{B} = \{B_1, 0, 0\}^t$. For the given deformation, the magnetic induction component in the chain direction is given as $B^c = \gamma B_1 / [1 + \gamma^2]$. The various components of stress are obtained as

$$\sigma_{11} = \frac{\mu_e}{2} [1 + \nu] \gamma^2 + \mu_e^c \left[1 - \frac{1}{[1 + \gamma^2]^{3/2}} \right] \gamma^2 + 4r[1 + \gamma^2] B_1^2 + 2\beta\gamma^4 B_1^2, \quad (6.17)$$

$$\sigma_{22} = -\frac{\mu_e}{2} [1 - \nu] \gamma^2 + \mu_e^c \left[1 - \frac{1}{[1 + \gamma^2]^{3/2}} \right] + 2\beta\gamma^2 B_1^2 \quad (6.18)$$

$$\text{and } \sigma_{12} = \mu_e \gamma + \mu_e^c \left[1 - \frac{1}{[1 + \gamma^2]^{3/2}} \right] \gamma + 2r\gamma B_1^2 + 2\beta\gamma^3 B_1^2. \quad (6.19)$$

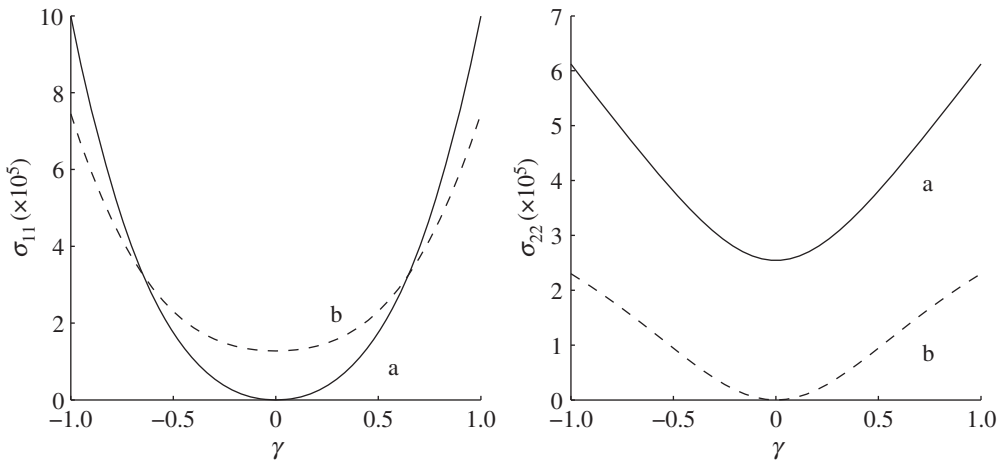


Figure 3. Normal stresses σ_{11} and σ_{22} (N m^{-2}) against the amount of shear γ for two directions of applied magnetic induction $\mathbb{B} = 0.2 \text{ T}$, $\mathbf{M} = \{0, 1, 0\}^t$. (a) $\mathbf{M} \parallel \mathbb{B}$ and (b) $\mathbf{M} \perp \mathbb{B}$.

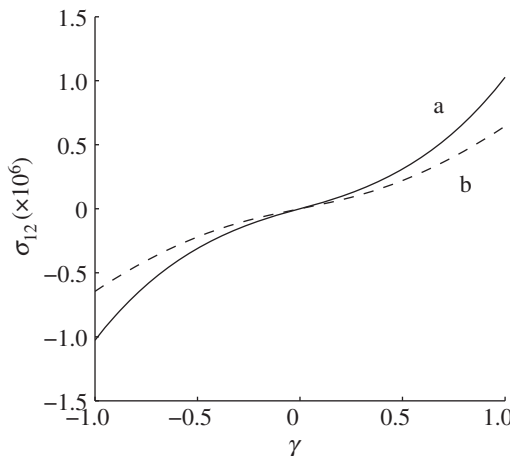


Figure 4. Shear stress σ_{12} (N m^{-2}) against the amount of shear γ for two directions of applied magnetic induction $\mathbb{B} = 0.2 \text{ T}$, $\mathbf{M} = \{0, 1, 0\}^t$. (a) $\mathbf{M} \parallel \mathbb{B}$ and (b) $\mathbf{M} \perp \mathbb{B}$.

The expressions for components of magnetic field are given by

$$h_1 = 2qB_1 + 2r[1 + \gamma^2]B_1 + 2\beta\gamma^2B_1 \quad (6.20)$$

and

$$h_2 = 2[r - q]\gamma B_1 + 2\beta\gamma B_1. \quad (6.21)$$

The extension of particle chains owing to shear deformation causes increments in all the three components of stress, the increase being zeroth order, linear and quadratic in γ for σ_{22} , σ_{12} and σ_{11} , respectively. The magnetic part of stress has a strong nonlinear coupling with the shear γ for the chosen material model, as can be seen in equation (6.14), for example. Variation of all the three components of stress are plotted with respect to the shear γ in figures 3 and 4. As $\gamma \rightarrow 0$, in the first case $h_1 \rightarrow 0$ while in the second case $h_2 \rightarrow 0$ and a linear constitutive relationship between magnetic field and magnetic induction is obtained.

The strong nonlinear coupling between chain anisotropy direction and deformation is evident from figure 3 where we observe that for small deformations, σ_{11} is higher when the particle chains

are perpendicular to the magnetic induction. This changes in the case of large deformations where a larger value of stress is obtained in the case when magnetic induction is applied in the direction of particle chains. Normal stress σ_{22} in the particle chain direction and the shear stress σ_{12} are, as expected, larger for the case when magnetic induction is applied in the direction of particle chains compared with the case when it is applied perpendicular to the chain direction. We also note that for the given magnetoelastic deformation, the magnitude of σ_{11} and σ_{12} is much higher than that of σ_{22} .

7. Numerical evaluations

We now present some numerical results corresponding to standard loading conditions to analyse the performance of our model. Several results corresponding to the variation of stress and magnetic field on static and dynamic magneto-mechanical loading conditions have been presented in a previous work for isotropic materials [25]. Hence in this section, we particularly focus on the effect of a directional anisotropy on the material response.

In addition to those given in equation (6.7), the following values of the material parameters are used for performing the computations

$$\left. \begin{aligned} \mu_v &= 5 \times 10^5 \text{ N m}^{-2}, & \mu_v^c &= 6 \times 10^5 \text{ N m}^{-2}, & r_v &= \frac{1}{\mu_0}, & q_v &= \frac{5}{\mu_0}, \\ \beta_v &= \frac{3}{\mu_0}, & T_m &= 5 \text{ s}, & T_v &= 100 \text{ s}, & T_m^c &= 2 \text{ s} & \text{ and } & T_v^c &= 50 \text{ s}. \end{aligned} \right\} \quad (7.1)$$

The parameters $\mu_v, r_v, q_v, T_m, T_v$ have been used by us in a previous work [25]. The parameters $\mu_v^c, \beta_v, T_m^c, T_v^c$ are nothing but the chain counterparts of μ_v, r_v, T_m and T_v , respectively, and are therefore assigned values with an order of magnitude same as them. The evolution laws (5.6)–(5.8) are integrated using the ode45 solver in Matlab which works using the Runge–Kutta method.

(a) No deformation, step magnetic induction

Let the anisotropy direction be given by $\mathbf{M} = \{1, 0, 0\}^t$ and a sudden magnetic induction $\mathbb{B} = \{B_1, B_2, 0\}^t$ is applied at time $t = 0$ at an angle ϕ to the chain direction \mathbf{M} while keeping the material undeformed ($\mathbf{F} = \mathbf{I}$). For these loading conditions, $B^c = B_1$ and the evolution equation (5.6) can be directly integrated to give

$$[\mathbb{B}_v]_1 = B_1 \left[1 - \exp\left(-\frac{\mu_0[q_v + r_v]t}{T_m}\right) \right] \quad \text{and} \quad [\mathbb{B}_v]_2 = B_2 \left[1 - \exp\left(-\frac{\mu_0[q_v + r_v]t}{T_m}\right) \right]. \quad (7.2)$$

The out of plane stress and magnetic field components vanish ($\sigma_{33} = h_3 = 0$) and the other components are given in the following form:

$$\sigma_{11} = [4r + 2\beta]B_1^2 + 4r_v B_1^2 \exp\left(-\frac{2\mu_0[q_v + r_v]t}{T_m}\right) + 2\beta_v B_1^2 \exp\left(-\frac{2t}{T_m^c}\right), \quad (7.3)$$

$$\sigma_{22} = 4rB_2^2 + 4r_v B_2^2 \exp\left(-\frac{2\mu_0[q_v + r_v]t}{T_m}\right), \quad (7.4)$$

$$\sigma_{12} = 4rB_1B_2 + 4r_v B_1B_2 \exp\left(-\frac{2\mu_0[q_v + r_v]t}{T_m}\right). \quad (7.5)$$

$$h_1 = 2[q + r + \beta]B_1 + 2[q_v + r_v]B_1 \exp\left(-\frac{\mu_0[q_v + r_v]t}{T_m}\right) + 2\beta_v B_1 \exp\left(-\frac{t}{T_m^c}\right) \quad (7.6)$$

and
$$h_2 = 2[q + r]B_2 + 2[q_v + r_v]B_2 \exp\left(-\frac{\mu_0[q_v + r_v]t}{T_m}\right). \quad (7.7)$$

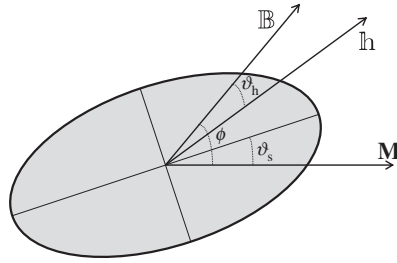


Figure 5. Principal directions of total Cauchy stress σ as principal axes of the ellipse, magnetic induction \mathbb{B} , magnetic field \mathbb{h} and anisotropy direction \mathbf{M} .

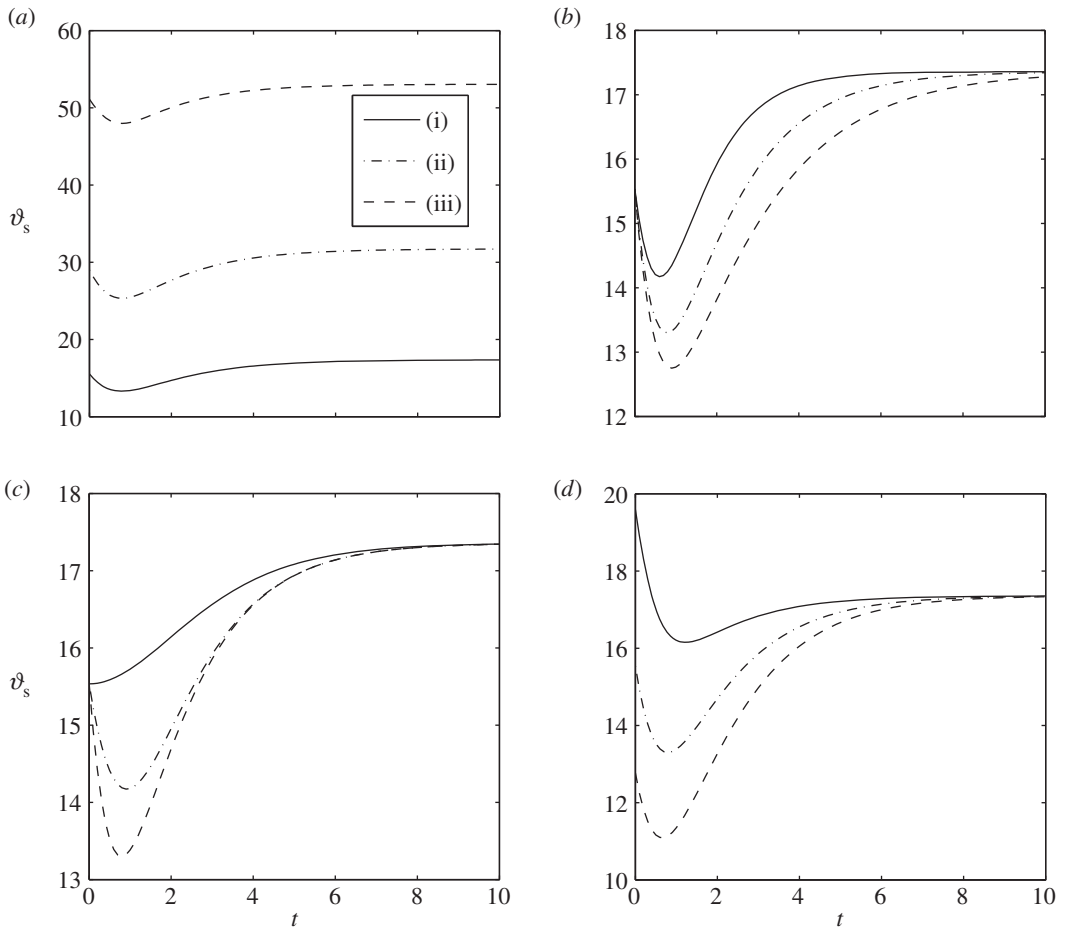


Figure 6. Angle ϑ_s (deg) versus time t (s). (a) (i) $\phi = \pi/6$, (ii) $\phi = \pi/4$, (iii) $\phi = \pi/3$; (b) $\phi = \pi/6$, (i) $T_m^c = 2s$, (ii) $T_m^c = 3s$, (iii) $T_m^c = 4s$; (c) $\phi = \pi/6$, (i) $q_v = 1/\mu_0$, (ii) $q_v = 3/\mu_0$, (iii) $q_v = 5/\mu_0$; (d) $\phi = \pi/6$, (i) $\beta_v = 1/\mu_0$, (ii) $\beta_v = 3/\mu_0$, (iii) $\beta_v = 5/\mu_0$.

In general, the principal directions of the stress are at an angle ϑ_s to the Cartesian basis vectors as shown in figure 5 and the angle ϑ_s keeps changing with the evolution of internal variables. The variation of ϑ_s with time is plotted in figure 6. Similarly, we define the angle between the magnetic field and the applied magnetic induction as ϑ_h and its evolution is plotted in figure 7. The

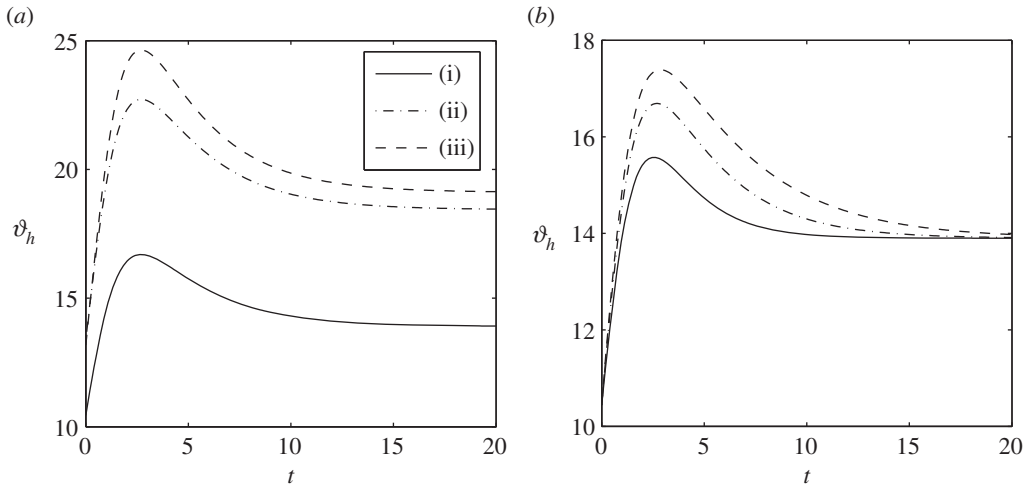


Figure 7. Variation of angle ϑ_h (deg) between magnetic field and magnetic induction with time t (s). (a) (i) $\phi = \pi/6$, (ii) $\phi = \pi/4$, (iii) $\phi = \pi/3$; (b) $\phi = \pi/6$, (i) $T_m^c = 2$ s, (ii) $T_m^c = 3$ s, (iii) $T_m^c = 4$ s.

computations are performed for a magnitude of the magnetic induction $|\mathbb{B}| = 0.5$ T and various values of the angle ϕ and the parameters T_m^c , q_v and β_v .

It is seen that starting from a non-zero value, ϑ_s first falls and then rises again to reach a steady value with time. This inflection point (minimum obtained by ϑ_s) may be attributed to the two different rates of evolution along the chain direction and along the direction of applied induction. The isotropic contribution from the stress relaxes faster causing the resultant principal stress to shift towards the chain direction and thereby reducing the value of ϑ_s . As the anisotropic contribution of stress also relaxes after some time, the resultant principal stress direction shifts away from the chain direction thereby increasing the value of ϑ_s , which then obtains a steady-state value. For an initial angle of $\phi = 30^\circ$ between applied magnetic induction and the particle chain direction, the maximum principal stress forms an angle of $\vartheta_s \sim 17.3^\circ$ with the chain direction at the steady state. The higher the initial angle ϕ between the magnetic induction and the chain direction, the higher is the angle of maximum principal stress. Increasing the values of either of the parameters T_m^c , q_v or β_v decreases the intermediate value of ϑ_s but eventually they reach the same equilibrium point.

Variation of the angle ϑ_h is slightly different where it first increases with time and then after obtaining a maximum, decreases to obtain an equilibrium value. The contribution of the magnetoelastic matrix to the magnetic field relaxes faster than that from the anisotropy direction, thereby causing the resultant magnetic field to tilt towards the chain direction and increasing the value of ϑ_h . It should be noted that the angle between the resultant magnetic field and the chain direction is given by $[\phi - \vartheta_h]$. As the magnetic field contribution from the chain direction also relaxes, the resultant field shifts away from the chain direction and the value of ϑ_h increases. The higher the initial angle ϕ of loading, the higher is the response ϑ_s . Increasing the value of parameter T_m^c causes a higher intermediate angle ϑ_h which finally evolves to reach the same equilibrium level. For the material parameters used, an initial angle $\phi = 30^\circ$ between magnetic induction and particle chain direction results in the magnetic field being generated at an angle $\vartheta_h \sim 13.9^\circ$ to the magnetic induction direction at the steady state.

(b) Pure shear

Consider a case where the particle chains are aligned at an angle ϕ with the unit vector \mathbf{e}_1 where $\{\mathbf{e}_1, \mathbf{e}_2, \mathbf{e}_3\}$ form an orthonormal basis of \mathbb{R}^3 . A magnetic induction $\mathbb{B} = \{B_1, 0, 0\}^t$ and a stretch

$\lambda_1 = \lambda$ are applied in the direction of \mathbf{e}_1 at $t = 0$ while λ_2 is held constant at unity. The deformation gradient tensor is given by

$$[\mathbf{F}] = \begin{bmatrix} \lambda & 0 & 0 \\ 0 & 1 & 0 \\ 0 & 0 & \frac{1}{\lambda} \end{bmatrix}, \quad (7.8)$$

while the vectors \mathbf{M} and \mathbf{m} are given by

$$\mathbf{M} = \frac{1}{\sqrt{1 + \tan^2 \phi}} \begin{bmatrix} 1 \\ \tan \phi \\ 0 \end{bmatrix} \quad \text{and} \quad \mathbf{m} = \frac{1}{\sqrt{1 + \tan^2 \phi}} \begin{bmatrix} \lambda \\ \tan \phi \\ 0 \end{bmatrix}. \quad (7.9)$$

Various quantities calculated for these deformation conditions are given by

$$\sigma_{33} = 0, \quad \lambda^c = \left[\frac{\lambda^2 + \tan^2 \phi}{1 + \tan^2 \phi} \right]^{1/2}, \quad B^c = \frac{\lambda^2 \sqrt{1 + \tan^2 \phi}}{\lambda^2 + \tan^2 \phi} B_1 \quad (7.10)$$

and

$$[\mathbf{g}] = \begin{bmatrix} \lambda^2 \cos^2 \phi & \lambda \sin \phi \cos \phi & 0 \\ \lambda \sin \phi \cos \phi & \sin^2 \phi & 0 \\ 0 & 0 & 0 \end{bmatrix}. \quad (7.11)$$

For these loading conditions, we define ϑ_s to be the angle between the direction of the maximum principal stress (σ_{\max}) and the basis vector \mathbf{e}_1 . The angle between the direction of the resultant magnetic field \mathfrak{h} and \mathbf{e}_1 is denoted as ϑ_h .

We now consider two separate cases—one with constant strain and time-varying magnetic induction and other with constant magnetic induction and time-varying strain.

(i) Magnetic induction rate

Let the material be pre-strained with a stretch $\lambda = 2$ such that the mechanical viscous effects have vanished when we start measuring the time at $t = 0$. At this instant, we gradually increase and then decrease the applied magnetic induction in the form shown in figure 8*a*. This corresponds to a magnetic induction rate of 0.8 T s^{-1} while the maximum value of magnetic induction reached is 0.8 T. We plot the evolution of σ_{\max} and ϑ_s with time in the same graph for two directions of the orientation of particle chains given by $\phi = \pi/6$ and $\phi = \pi/4$.

It is seen from figure 8*b,c* that the principal stress first increases and then decreases with time following the applied magnetic induction. It is interesting to note the evolution of ϑ_s in this case which first starts from a high value, falls down to a minimum and then rises again to reach a steady value. This essentially means that the axes of principal stresses keeps rotating with time owing to different behaviour of the material along the anisotropy direction as compared with the general isotropic behaviour. Initially, most of the stress is undertaken by the anisotropy direction (hence the high value of ϑ_s) which is gradually transferred to the bulk material when B_1 rises and ϑ_s falls. As B_1 falls again, ϑ_s rises because the majority of stress is regained by the anisotropy direction. For the combination of parameters chosen, the maximum value of σ_{\max} reached is higher for the smaller value of angle ϕ between the loading and the chain directions. Also the steady state value of ϑ_s is different from the value of ϕ which implies that the principal stress directions are in general different from the directions of anisotropy and the applied deformation. When the magnetic induction is turned off at time $t = 2 \text{ s}$, a discontinuity in the slope of σ_{\max} is observed and the stress decay is faster after that point.

The total magnetic field $|\mathfrak{h}|$, as can be seen in figure 8*d,e*, also increases and then falls with time following the applied magnetic induction. The interesting feature to note is the sudden rise in the total magnetic field $|\mathfrak{h}|$ and the angle ϑ_h as $B_1 \rightarrow 0$. On the application of a magnetic induction, the material develops a magnetization in the direction of applied \mathfrak{b} and as B_1 is switched off, the magnetization is still non-zero and decays gradually. As a result, a magnetic field \mathfrak{h} is developed

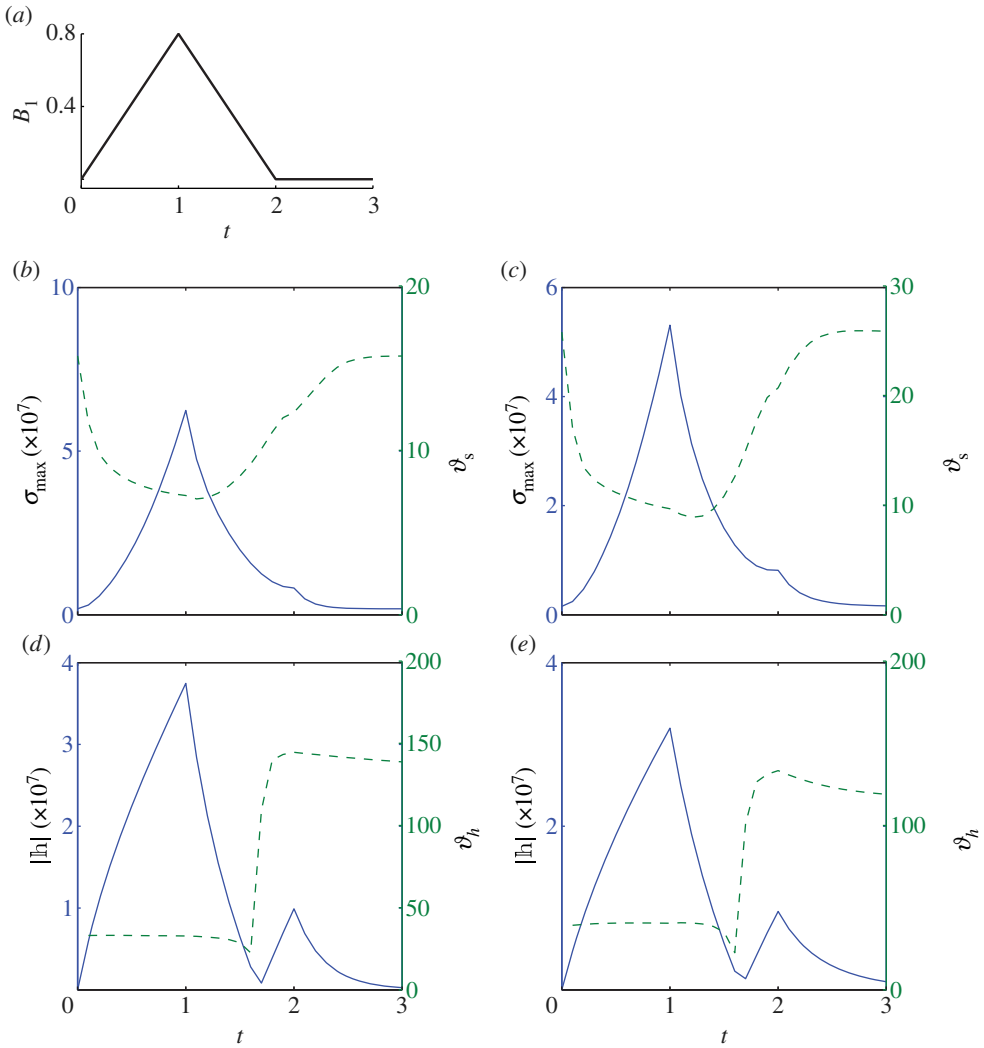


Figure 8. (a) Applied magnetic induction at $\pm 0.8 \text{ T s}^{-1}$. Maximum principal stress σ_{\max} (N m^{-2}) and its direction ϑ_s (deg) versus time (s) for two values of angle ϕ : (b) $\phi = \pi/6$ and (c) $\phi = \pi/4$. Magnetic field $|\mathbb{h}|$ (A m^{-1}) and its angle ϑ_h (deg) versus time (s) for two values of angle ϕ : (d) $\phi = \pi/6$ and (e) $\phi = \pi/4$. Solid curves correspond to σ_{\max} in (b,c) and $|\mathbb{h}|$ in (d,e); dotted curves correspond to ϑ_s in (b,c) and ϑ_h in (d,e). (Online version in colour.)

in the material in the opposite direction to counter the effect of \mathbb{m} in order to balance the constitutive relation (3.2). This effect can be seen at $t = 2 \text{ s}$ in figure 8d,e. We observe a rise in $|\mathbb{h}|$ and a huge rise in ϑ_h which essentially means that the total magnetic field has changed direction.

(ii) Strain rate

Let the material be pre-magnetized with a magnetic induction of $B_1 = 0.5 \text{ T}$ such that the magnetic viscous effects have vanished when we start measuring the time at $t = 0$. At this instant, we gradually increase and then decrease the applied strain λ in the form shown in figure 9a. This corresponds to a strain rate of 0.8 s^{-1} while the maximum value of the stretch λ reached is 3. The evolution of σ_{\max} , $|\mathbb{h}|$, ϑ_s and ϑ_h is shown with time.

The maximum principal stress σ_{\max} rises and falls following the increase and decrease of λ . Starting from a non-zero, although small, value due to magnetic contribution of stress, it reaches a maximum and then sharply falls down to the same equilibrium value. The maximum value

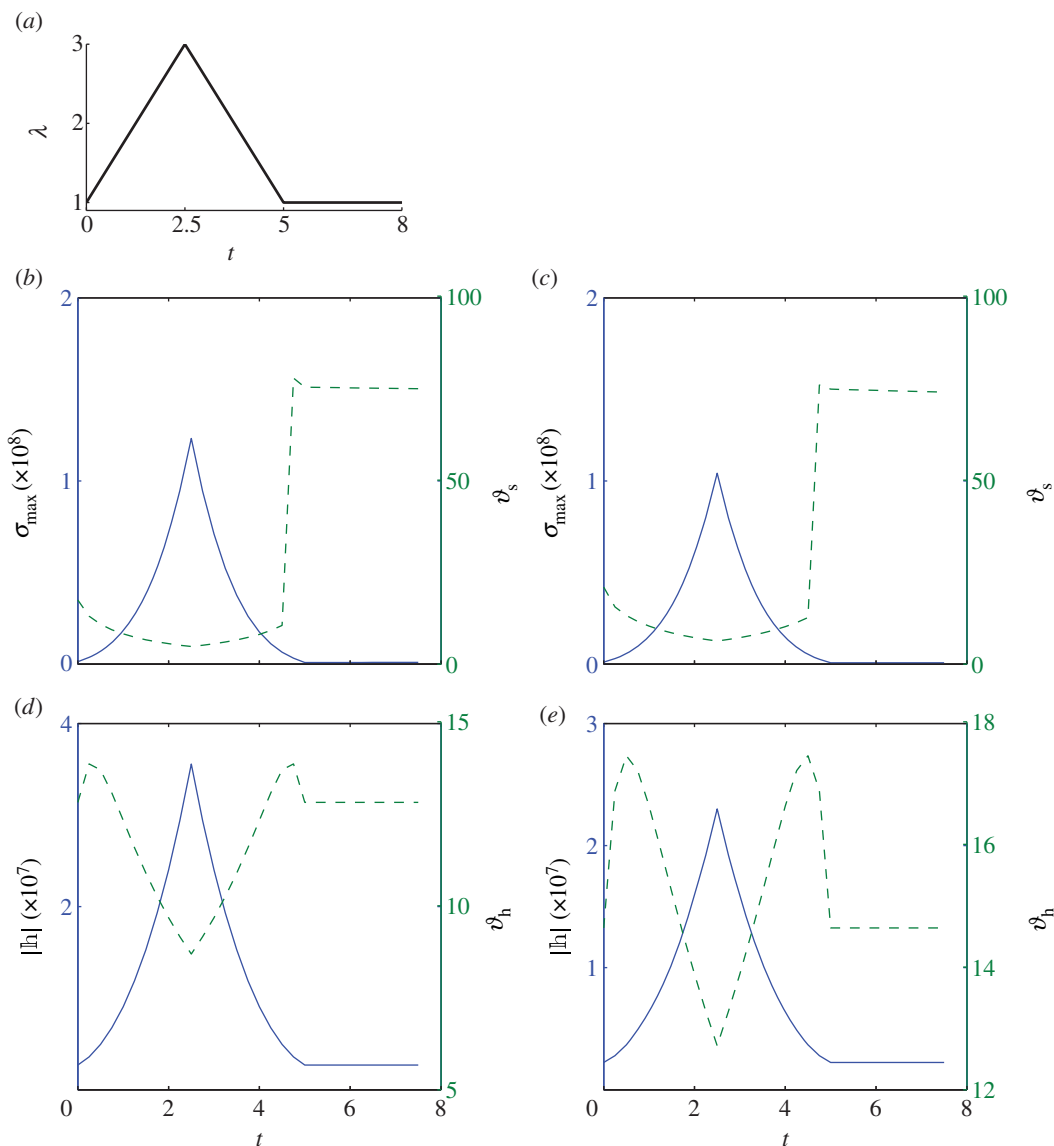


Figure 9. (a) Applied strain at $\pm 0.8 \text{ s}^{-1}$. Maximum principal stress σ_{\max} (N m^{-2}) and its angle ϑ_s (deg) versus time (s) for two values of the angle ϕ : (b) $\phi = \pi/6$ and (c) $\phi = \pi/4$. Magnitude of magnetic field $|h|$ (A m^{-1}) and its angle ϑ_h (deg) versus time (s) for two values of the angle ϕ : (d) $\phi = \pi/6$ and (e) $\phi = \pi/4$. Solid curves correspond to σ_{\max} in (b,c) and $|h|$ in (d,e); dotted curves correspond to ϑ_s in (b,c) and ϑ_h in (d,e). (Online version in colour.)

reached is higher for smaller value of ϕ or when the angle between anisotropy and loading direction is small.

The orientation ϑ_s of the maximum principal stress starts from a non-zero value, decreases to reach a minimum and then rises again with time. As the stretch is reduced to 1 when $t \rightarrow 5$ s, the direction of maximum principal stress changes rapidly due to which we observe a jump in the value of ϑ_s . The angle ϑ_s is also slightly larger for the case of smaller ϕ .

The magnetic field $|h|$, like in the previous case, first increases and then decreases with time following the change in λ . The evolution of magnetic field stops as soon as the changes in λ are ceased because h has no dependence on C_V as can be seen from equation (5.16). A smaller value of ϕ leads to a higher maximum value obtained by h_{tot} . The angle ϑ_h increases with time slightly

and then falls to a minimum, it then increases again falling back to the steady state. Thus, for the chosen material parameters, the effective magnetic field direction keeps changing quite rapidly with time.

8. Concluding remarks

In this paper, we have proposed a procedure to model nonlinear magneto-viscoelastic deformations for polymers with a transverse isotropic arrangement of magnetic particle chains. An additional deformation gradient \mathbf{F}^c and an additional magnetic induction \mathbb{B}^c are defined in the particle chain direction. Following the ideas in [25], they are then decomposed into equilibrium and non-equilibrium parts to consider the dissipation effects. A further decomposition of the free energy into isotropic elastic, isotropic viscous, anisotropic elastic and anisotropic viscous parts is performed to simplify the problem. It is observed that this decomposition yields very clear expressions for the total Cauchy stress and the magnetic field. This approach towards modelling anisotropy in magnetoelasticity is different from that proposed by Bustamante [33], but it gives rather simpler expressions and fewer material parameters. Physically reasonable and thermodynamically consistent free energy density functions and evolution laws are proposed in order to obtain illustrative solutions to some simple problems. Analytical expressions for the total Cauchy stress and the magnetic field are computed for non-dissipative magnetoelastic deformations that show the effect of the anisotropy direction on material response.

It is interesting to observe that the principal stress directions and the direction of the resulting magnetic field are in general different from the loading directions owing to the inherent anisotropy in the material. As is seen from, for example, figures 6 and 7, these directions change with time owing to evolution of the internal variable. The evolution strongly depends on the material parameters T_m^c , q_v , β_v , the angle ϕ between magnetic induction and chain direction as well as the rate of applied magnetic induction and strain. Possibility of existence of more physically reasonable constitutive relations (by matching with experimentally obtained data) and solutions of several boundary value problems using numerical computations will be studied in forthcoming papers.

Acknowledgement. The authors also thank Mr. Bastian Walter for preparation of MRE samples and providing corresponding SEM images used in figure 1.

Funding statement. This work is supported by an advanced investigator grant from the European Research Council towards the project MOCOPLY.

References

- Galipeau E, Castaneda PP. 2013 Giant field-induced strains in magnetoactive elastomer composites. *Proc. R. Soc. A* **469**, 20130385. (doi:10.1098/rspa.2013.0385)
- Yalcintas M, Dai H. 2004 Vibration suppression capabilities of magnetorheological materials based adaptive structures. *Smart Mater. Struct.* **13**, 1–11. (doi:10.1088/0964-1726/13/1/001)
- Varga Z, Filipcsei G, Zrinyi M. 2006 Magnetic field sensitive functional elastomers with tuneable elastic modulus. *Polymer* **47**, 227–233. (doi:10.1016/j.polymer.2005.10.139)
- Böse H, Rabindranath R, Ehrlich J. 2012 Soft magnetorheological elastomers as new actuators for valves. *J. Intell. Mater. Syst. Struct.* **23**, 989–994. (doi:10.1177/1045389X11433498)
- Jolly MR, Carlson JD, Muñoz BC. 1996 A model of the behaviour of magnetorheological materials. *Smart Mater. Struct.* **5**, 607–614. (doi:10.1088/0964-1726/5/5/009)
- Boczkowska A, Awietjan SF. 2009 Smart composites of urethane elastomers with carbonyl iron. *J. Mater. Sci.* **44**, 4104–4111. (doi:10.1007/s10853-009-3592-7)
- Landau LD, Lifshitz EM. 1960 *Electrodynamics of continuous media*. Oxford, UK: Pergamon Press.
- Livens GH. 1962 *The theory of electricity*, 2nd edn. Cambridge, UK: Cambridge University Press.
- Tiersten HF. 1964 Coupled magnetomechanical equations for magnetically saturated insulators. *J. Math. Phys.* **5**, 1298–1318. (doi:10.1063/1.1704239)

10. Brown WF. 1966 Magnetoelastic interactions. Springer tract in natural philosophy (ed. C Truesdell). Berlin, Germany: Springer.
11. Maugin GA, Eringen AC. 1972 Deformable magnetically saturated media. I. Field equations. *J. Math. Phys.* **13**, 143–155. (doi:10.1063/1.1665947)
12. Maugin GA, Eringen AC. 1972 Deformable magnetically saturated media. II. Constitutive theory. *J. Math. Phys.* **13**, 1334–1347. (doi:10.1063/1.1666143)
13. Maugin GA, Eringen AC. 1977 On the equations of the electrodynamics of deformable bodies of finite extent. *J. Mec.* **16**, 101–146.
14. Pao YH. 1978 Electromagnetic forces in deformable continua. In *Mechanics today*, vol. 4 (ed. S Nemat-Nasser), pp. 209–305. Oxford, UK: Oxford University Press.
15. Eringen AC, Maugin GA. 1990 *Electrodynamics of continua*, vol. 1. New York, NY: Springer.
16. Brigadnov IA, Dorfmann A. 2003 Mathematical modeling of magneto-sensitive elastomers. *Int. J. Solids Struct.* **40**, 4659–4674. (doi:10.1016/S0020-7683(03)00265-8)
17. Dorfmann A, Ogden RW. 2003 Magnetoelastic modelling of elastomers. *Eur. J. Mech. A* **22**, 497–507. (doi:10.1016/S0997-7538(03)00067-6)
18. Kankanala SV, Triantafyllidis N. 2004 On finitely strained magnetorheological elastomers. *J. Mech. Phys. Solids* **52**, 2869–2908. (doi:10.1016/j.jmps.2004.04.007)
19. Dorfmann A, Ogden RW. 2004 Nonlinear magnetoelastic deformations. *Q. J. Mech. Appl. Math.* **57**, 599–622. (doi:10.1093/qjmam/57.4.599)
20. Bustamante R, Dorfmann A, Ogden RW. 2007 A nonlinear magnetoelastic tube under extension and inflation in an axial magnetic field: numerical solution. *J. Eng. Math.* **59**, 139–153. (doi:10.1007/s10665-006-9088-4)
21. Otténio M, Destrade M, Ogden RW. 2008 Incremental magnetoelastic deformations, with application to surface instability. *J. Elast.* **90**, 19–42. (doi:10.1007/s10659-007-9120-6)
22. Saxena P, Ogden RW. 2012 On Love-type waves in a finitely deformed magnetoelastic layered half-space. *Z. Angew. Math. Phys.* **63**, 1177–1200. (doi:10.1007/s00033-012-0204-1)
23. Steigmann DJ. 2009 On the formulation of balance laws for electromagnetic continua. *Math. Mech. Solids* **14**, 390–402. (doi:10.1177/1081286507080808)
24. Maugin GA. 2009 On modelling electromagnetomechanical interactions in deformable solids. *Int. J. Adv. Eng. Sci. Appl. Math.* **1**, 25–32. (doi:10.1007/s12572-009-0002-y)
25. Saxena P, Hossain M, Steinmann P. 2013 A theory of finite deformation magneto-viscoelasticity. *Int. J. Solids Struct.* **50**, 3886–3897. (doi:10.1016/j.ijsolstr.2013.07.024)
26. Lubliner J. 1985 A model of rubber viscoelasticity. *Mech. Res. Commun.* **12**, 93–99. (doi:10.1016/0093-6413(85)90075-8)
27. Reese S, Govindjee S. 1998 A theory of finite viscoelasticity and numerical aspects. *Int. J. Solids Struct.* **35**, 3455–3482. (doi:10.1016/S0020-7683(97)00217-5)
28. Maugin GA, Sabir M, Chambon P. 1987 Coupled magnetomechanical hysteresis effects: application to nondestructive testing. In *Electromagnetomechanical interactions in deformable solids and structures (IUTAM, Tokyo, 1986)* (eds Y Yamamoto, K Miya), pp. 255–264. Amsterdam, The Netherlands: North-Holland.
29. Spencer AJM. 1971 Theory of invariants. In *Continuum physics*, vol. I (ed. AC Eringen), pp. 239–353. New York, NY: Academic.
30. Zheng Q-S. 1994 Theory of representations for tensor functions: A unified invariant approach to constitutive equations. *Appl. Mech. Rev.* **47**, 545–587. (doi:10.1115/1.3111066)
31. Shams M, Destrade M, Ogden RW. 2011 Initial stresses in elastic solids: constitutive laws and acoustoelasticity. *Wave Motion* **48**, 552–567. (doi:10.1016/j.wavemoti.2011.04.004)
32. Holzapfel GA, Gasser TC. 2001 A viscoelastic model for fiber-reinforced composites at finite strains: continuum basis, computational aspects and applications. *Comput. Methods Appl. Mech. Eng.* **190**, 4379–4403. (doi:10.1016/S0045-7825(00)00323-6)
33. Bustamante R. 2010 Transversely isotropic nonlinear magneto-active elastomers. *Acta Mech.* **210**, 183–214. (doi:10.1007/s00707-009-0193-0)
34. Danas K, Kankanala SV, Triantafyllidis N. 2012 Experiments and modeling of iron-particle-filled magnetorheological elastomers. *J. Mech. Phys. Solids* **60**, 120–138. (doi:10.1016/j.jmps.2011.09.006)
35. Shariff MHB. 2008 Nonlinear transversely isotropic elastic solids: an alternative representation. *Q. J. Mech. Appl. Math.* **61**, 129–149. (doi:10.1093/qjmam/hbm028)
36. Destrade M, Donald BM, Murphy JG, Saccomandi G. 2013 At least three invariants are necessary to model the mechanical response of incompressible, transversely isotropic materials. *Comput. Mech.* **52**, 959–969. (doi:10.1007/s00466-013-0857-4)

37. Vergori L, Destrade M, McGarry P, Ogden RW. 2013 On anisotropic elasticity and questions concerning its finite element implementation. *Comput. Mech.* **52**, 1185–1197. (doi:10.1007/s00466-013-0871-6)
38. Srinivasa AR. 2012 On the use of the upper triangular (or QR) decomposition for developing constitutive equations for Green-elastic materials. *Int. J. Eng. Sci.* **60**, 1–12. (doi:10.1016/j.ijengsci.2012.05.003)
39. Klinkel S, Sansour C, Wagner W. 2004 An anisotropic fibre-matrix material model at finite elastic-plastic strains. *Comput. Mech.* **35**, 409–417. (doi:10.1007/s00466-004-0629-2)
40. Nedjar B. 2007 An anisotropic viscoelastic fibre-matrix model at finite strains: continuum formulation and computational aspects. *Comput. Methods Appl. Mech. Eng.* **196**, 1745–1756. (doi:10.1016/j.cma.2006.09.009)
41. Maugin GA. 1988 *Continuum mechanics of electromagnetic solids*. Amsterdam, The Netherlands: North-Holland.
42. Koprowski-Theiss N, Jöhlitz M, Diebels S. 2011 Characterizing the time dependence of filled EPDM. *Rubber Chem. Technol.* **84**, 147–165. (doi:10.5254/1.3570527)
43. Lion A. 1997 A physically based method to represent the thermo-mechanical behaviour of elastomers. *Acta Mech.* **123**, 1–25. (doi:10.1007/BF01178397)